ANTAL KERPELY DOCTORAL SCHOOL OF

MATERIAL SCIENCE AND TECHNOLOGY

The recovery of pure Zn from spent pickling liquor by combining electrowinning and anion-exchange separation process

A dissertation submitted in partial fulfilment of the requirements for
the degree of Doctor of Philosophy in Chemical Metallurgy as a part of
Stipendium Hungaricum Scholarship in
Material Science and Technology

By

Hanna Zakiyya, MT (Indonesia)

Supervisor:

Prof. Dr. Tamás Kékesi, DSc

Head of the Doctoral School:

Prof. Dr. Valéria Mertinger, DSc

Institute of Chemical Metallurgy and Foundry Engineering
Faculty of Materials and Chemical Engineering
University of Miskolc
Miskolc, Hungary

2024

Synopsis

A great amount of metals (mainly Zn and Fe) are dissolved in the hydrochloric Spent Pickling Liquor (SPL) generated by the surface cleaning technology applied before hot dip galvanization. The Zn concentration can reach especially high levels if the recycled faulty objects are de-zinced in stripping lines. In order to extract the valuable zinc content, a comprehensive purification procedure has been devised.

Anion-exchange separation based on the different tendencies in the formation of chloro-complex ions could serve as an efficient method. The chromatographic setup allows the utilization of even minute differences in the distribution functions expressing the behaviour patterns according to the variation in the free chloride ion concentration. As determined by the equilibrium studies, iron, as the major impurity, can be removed in its lower oxidation state directly upon the loading and the first rinsing of the chromatographic column holding the strongly basic anion-exchange resin together with the impurities incapable of forming stable anionic chloro-complex species (Al, Mn, Ni and Co). Even though most of the Fe is in the reduced Fe(II) form in the SPL – reacted with the iron surface and the sludge particles – the process still includes a reducing pre-treatment by inducing com-proportionation to assure the uniform ferrous state. Among the practical impurities the separation of only Pb is incomplete, but it can no longer exist in the industrial stream of galvanizing industries in the EU. Although, minor quantities of Cu and Fe may still remain in the final solution, a cementation or pre-deposition technique may eliminate the residues of these more noble contaminants. The equilibrium studies of the anion-exchange distribution in NaCl solutions showed similar tendencies to those already known in HCl media. The anion-exchange chromatographic separation was devised – with the finer tuning of the parameters – according to the specific equilibrium and kinetic experimental results. The best practical loading volume was found close to the gross volume of the resin bed if higher flow rates (3 – 4 BV/h) are to be applied. Besides the extremely high elimination ratios of the important impurities, about 97% of Zn can be obtained in the main eluate by applying the optimized sequence.

To attain a satisfactory cathodic deposition of zinc from the purified chloride solution, it is essential to appropriately adjust the main parameters. The provide a sufficient concentration of Zn, the accurate control of pH, and the selection of the correct range of current density are indispensable requirements in an open cell, while the main impurity, iron can change the conditions by intensifying the evolution of hydrogen even at less than 1 g/dm^3 concentrations. Similar effects of minor Ni contamination were pointed out. The role of these practical parameters and that of the application of electrolyte agitation on the cathodic process could be revealed by the potentiodynamic experiments.

The long-term electrolysis was efficient with Zn concentrations higher than 50 g/dm^3 with relatively high (600 – 1200 A/m^2) apparent (geometric) current densities and ~ pH 3 applied. At as low as 10 g/dm^3 Zn-concentration, no conditions were found suitable to produce acceptable morphologies of the deposit. At higher apparent current densities than 1000 A/m^2, the reduction of the H^+ ions also resulted in strong increasing pH values leading to considerable hydroxide precipitations. The addition of NaCl could result in complex effects. While the Na^+ ions could mitigate the rough crystal structures, the increasing salt concentration inhibited the transport process and enhanced dendritic crystal growth.

1 Introduction

One of the most common corrosion control methods is coating the steel surface with a passivating layer, like in the case of hot dip galvanizing (HDG), where a thick zinc coating

protects the surface of the steel objects. However, the steel surface usually exhibits scaling and corrosion, making direct Zn coating impossible. Surface cleaning is an important preparatory procedure. Thus, HDG technology, as illustrated by Fig. 1, may produce wastes too and cause severe environmental hazards [1] [2] [3].

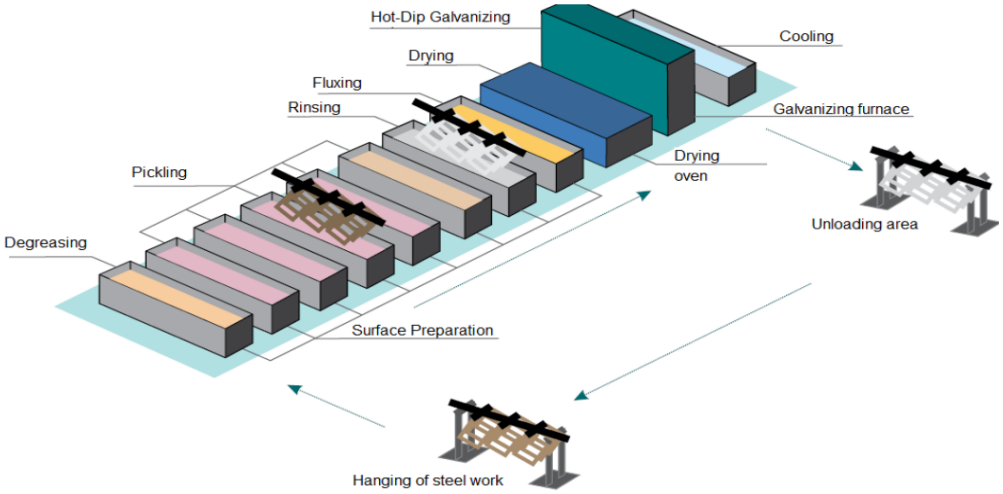

Fig. 1 The main units of hot dip galvanizing plants using the dry batch technology [4].

The pickling step is also used to remove faulty Zn coatings from the recycled objects. Generally, acidic media are applied. The object is immersed or end-to-end passed through a acid solution in which magnetite, hematite, wustite, minor oxide constituents, or recycled Zn layers react with hydrogen ions in the bath [5]. If the faulty zinc layer is removed in a separate "stripping" line, like in most modern technologies, usually a special SPL (stripping solution) of remarkably high Zn concentration arises associated with considerably lower iron content.

Known for its superiority in maintaining the adherence of the galvanic coating and lowering the possibility of localized corrosion, HCl is preferably used as the pickling agent [6] [7] [8]. Furthermore, it offers faster pickling, easier cleaning, lower acid and heat consumption, and less liquid waste.

The reagent loses its efficiency after decreasing its initial HCl concentration by 75-85% [5] [9]. The dominant components of the spent chloride acid solution are $ZnCl_2$, $FeCl_2$, and HCl, in this molar order if it arises from the stripping line. In this case, the exhausted solution would be highly rich in zinc in the range of 80–230 g/dm^3, and low in Fe (about 5–20 g/dm^3) along with the remaining active HCl of about 5–30 g/dm^3 concentration. If however the spent liquor comes from the main production line treating basically the previously uncoated metal, the composition may vary as 100–160 g/dm^3 of Fe, 5–20 g/dm^3 of Zn and 20–50 g/dm^3 of HCl [10] [11] [12]. Therefore, this research is oriented mainly towards the former type of SPL, coming from the stripping lines of modern galvanizing plants. As impurities, this solution may also contain trace amounts of other metals such as manganese, lead, aluminium, chromium, cadmium, nickel, copper, and cobalt, totalling in the range below 1 g/dm^3 [13] [14].

Given the contained heavy metals and the corrosive nature, the SPL is categorized as a complex hazardous waste by the EU Waste Framework [6] [15] [16] [17] [18]. In addition, according to the circular economic strategies, SPL can be considered as a secondary source of Zn, and also Fe. The recovery of these metallic values may be economical even without the legal encouragement if the purity of the recycled metal reaches levels beyond the ordinary technical grades. Thus recycling SPL may be directly in line with the relevant EU regulations and also with economic aspirations if an efficient procedure is devised producing pure Zn as the main product [13] [19]. Additionally, the Bureau of International Recycling mentioned that

producing Zn and Fe from secondary raw materials may affect CO_2 saving by great ratios [19]. If however the SPL is not recycled, just neutralized and a heterogeneous waste mass is disposed of, the allowed concentration of metals and chloride ions is strictly regulated in Europe, and similarly elsewhere [20]. As with all metals, the price of zinc strongly depends on purity. For example, the 99.999% (5N) purity zinc (available as a special material) may cost almost 20 – 100 times more than the common commodity at the metal markets [21]. High purity zinc can be used for producing semiconductor compounds, such as CdZnTe for detectors, ZnSe for blue light emitting diodes, ZnTe for thermo-electric cooling devices and doping semiconductors to make p-type [22]. Even though nanomaterials/powders production from secondary resources has gained considerable attention, the research for this production from spent pickling liquor is still limited to iron nanomaterial. Preparing ZnO nanoparticles from ultra-pure Zn metal is also extensively popular as it has excellent optical, electrical, and electrochemical super capacitor, thermal properties, and catalytic activities and is economically favourable [23]. In addition, using pure zinc in preparing biodegradable material, mainly in bone and blood vessels, has increased significant interest [24]. Therefore, reaching a high purity in the recovered is the main goal of the envisaged research challenge.

2 Experimental procedures

2.1. The anion-exchange chromatographic separation

The resin was physically purified and then conditioned in the chloride form, then fed into the glass chromatographic column, and the procedure started according to the scheme shown in Fig. 2. The flow rate was set at 1.5 ~ 1.7 bed volumes per hour (BV), as lower than the 3 BV usually applied value in practice, to enhance separation but still allow acceptable productivity.

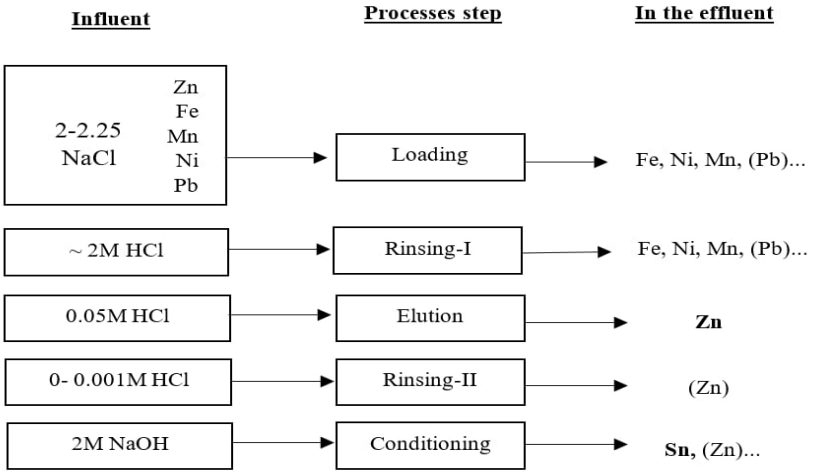

Fig. 2 A possible method for the anion exchange purification of Zn in HCl solutions effecting the separation of Fe and the practically important minor impurities.

After the delicate steps, the rinsing flow rate was raised to ~ 3 BV. Effluent samples (10 cm^3 each) were collected regularly during the procedure.

The liquid level in the chromatographic columns – of 2.5 cm inner diameter and 25 cm effective height - was kept at approx. 3 cm higher than the resin bed. It prevented any disturbance of the top layer as the influent solution was fed drop-by-drop from the overhead vessel, avoiding also any accidental inclusion of air bubbles. Glass beads were placed on the top of the resin, separated by a layer of glass wool to prevent the floating of the resin when denser solutions were fed. Operating conditions can be seen in Fig. 3.

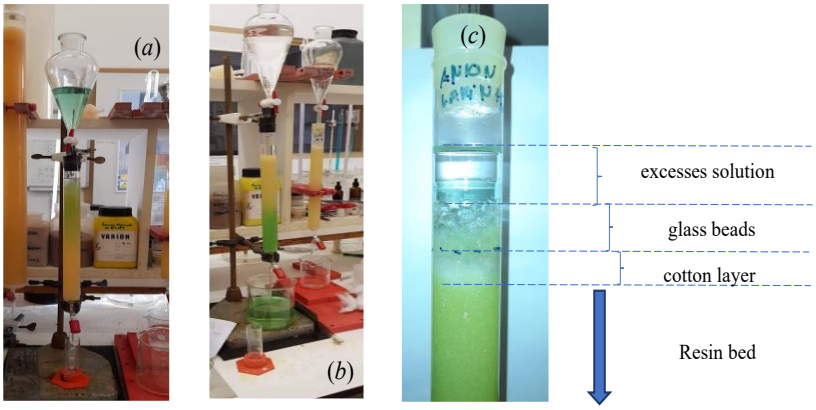

Fig. 3 The loading (a) and the rinsing (b) stages of a chromatographic separation process, and the arrangement of the upper part of the resin bed in the column(c).

During the critical phases of the procedure, the flow was set lower than usually applied to achieve a better separation but it was raised to the normal ~ 3 BV/h for the later parts of the rinsing steps. The composition of model solutions containing Zn, Fe, and other impurity elements was as specified in Table 1.

Table 1 Composition of the loaded solutions

Cl^- (M)	Zn (g/dm^3)	Fe(II) (g/dm^3)	Other impurity elements (mg/dm^3)						
			Mn	Ni	Sn	Cu	Al	Pb	Co
6.5	25	140	~ 500	~ 500	~ 500	~ 500	~ 500	~ 500	~ 500

The procedure was started by loading 100 cm^3, 2 M HCl blank solution to the column to set the Cl^- ion concentration to the starting value in the void fraction of the bed. It was followed by loading the prepared solution (100 cm^3) of the same free Cl^- ion concentration but containing the metals too. In the rinsing step, 200 cm^3 2M of NaCl was applied to remove all the Fe(II) from the column. Elution of Zn was carried out by slightly acidified solutions, containing low concentration (0.05 – 0.2 M) HCl. The conditioning step was devised to remove the residual strongly sorbed elements with 300 cm^3 of 2M NaOH. Effluent solution samples (10 cm^3 each) were collected regularly at fixed intervals to be analysed by AAS.

2.2 Potentiodynamic experiments

The initial cathode was a copper plate with an active surface area of 2 cm^2, surrounded by polyethylene masking. A thin layer of Zn was pre-deposited on the active electrode surface, then polished with SiC sandpaper of 800 grit, rinsed with distilled water and acetone, and finally dried to create a uniform surface before installation into the cell. In order to avoid changes in the conditions of the electrolyte, and to avoid the interference by the anodic gas evolution at the reduction process, a pure zinc anode was used as the counter electrode. The potentiodynamic investigations were conducted using freshly prepared solutions for experimental cycles examining various effects in the same concentration of the electrolyte. The saturated calomel reference electrode (SCE) was connected to the cathode (work electrode) surface via a tube bridge with a Lugging-capillary tip (~ 1 mm diameter) filled with the electrolyte solution. All tests were conducted at room temperature with a continuous polarization, applying a speed of 40 mV/s and a sampling rate of 10/s. The cell was connected to a computer-controlled potentiostat, developed at our laboratory. Due to the remarkable changes of the surface structure, the uncertain actual current densities could not be expressed. Therefore, the actual current readings were recorded and plotted, without dividing with the

initial (geometric) surface area. This approach emphasizes the importance of the often dramatically changing deposit morphology. The specially developed software controlled the potentiostat and recorded the results using the NI LabView platform. The surface structures were photographed through the glass walls during the polarization process. The potentiodynamic setup is shown is Fig. 4.

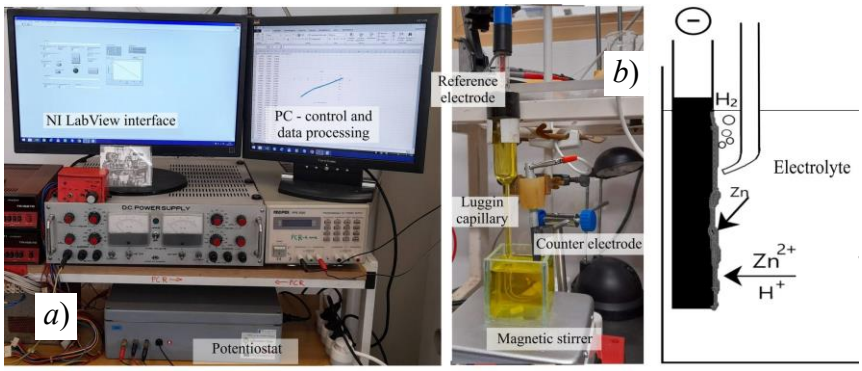

Fig. 4 Potentiodynamic equipment (a), electrochemical cell (b) and the illustration c) the working electrode (c).

2.3 Galvanostatic experiments

Galvanostatic tests were conducted with constant current settings corresponding to initial current densities of 150 - 4800 A/m^2 at the prepared active cathode surface of 4 cm^2. The actual current densities may become considerably lower in cases of the irregular electro-crystallization and the usual surface roughening. The electrolysis was carried out with freshly prepared electrolyte solutions in parallel setups by applying various power supplies of precise analogue regulation and connected multimeter units (Fig. 5).

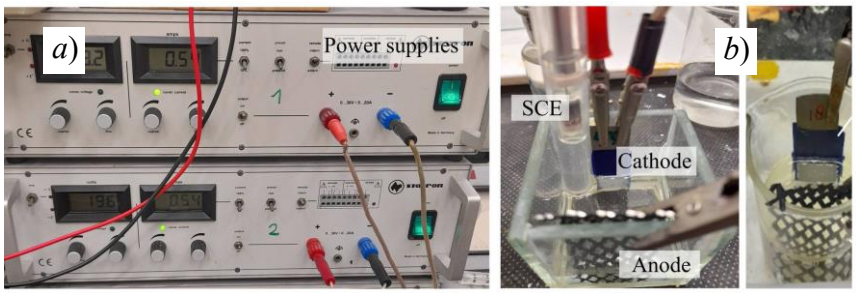

Fig. 5 Galvanostatic power supplies (a) and the experimental cell (b).

In order to simulate the practical conditions, the counter electrode used in galvanostatic studies was made of an inert - dimensionally stable anode (DSA) – mesh material. The electric parameters and the pH were monitored during the electrowinning runs. Table 2 summaries the studied variables.

Table 2 The examined ranges of the variables

Potentiodynamic			
Zn conc., g/dm^3		pH	Agitation
30, 60, 90, 120, 150		1.5; 2; 3; 4.5	50 -500 r.p.m.
Galvanostatic			
Zn conc., g/dm^3	pH	NaCl conc., g/dm^3	Apparent current density (c.d.) , A/m
6, 12.5, 25, 50, 100	0; 1; 2; 5	0, 1, 2, 4, 6	150, 300, 600, 1200, 2400, 4800

Electrolyte samples (0.5 cm^3) taken from the cell were analyzed by atomic absorption spectrophotometry (AAS) and the pH was monitored. The change in macro-structures of the deposit was evaluated by the optical microscopic photographs of the cathode surface. In order to determine the current efficiency of Zn deposition, the changes in the cathode mass (Δm) and in the Zn concentration (Δc) were measured. The current efficiencies (c.e.) were expressed as the ratios of the useful and the total electric charges measured:

$$c.e. = \frac{n\ \mathrm{F}\,\Delta m}{I\ \Delta t\ \mathrm{M_{Zn}}} \approx \frac{n\ \mathrm{F}\,V_S \Delta c}{I\ \Delta t\ \mathrm{M_{Zn}}} \quad \text{.....(6)}$$

where n is the effective unit charge of the electroactive ions, M_{Zn} is the molar mass, F is Faraday's constant, and I is the applied and recorded electric current. Due to the difficulty of rinsing and drying the loose deposits accurately, especially those obtained with the addition of NaCl, the concentration results were found more reliable to be used for this purpose.

3 Results and discussions

3.1 The separation scheme

The most common concentration of Zn and pH in the SPL was set in the raw solution. Figures 6 and 7 show the separation of Zn from Fe, and also from the rest of the practical impurities.

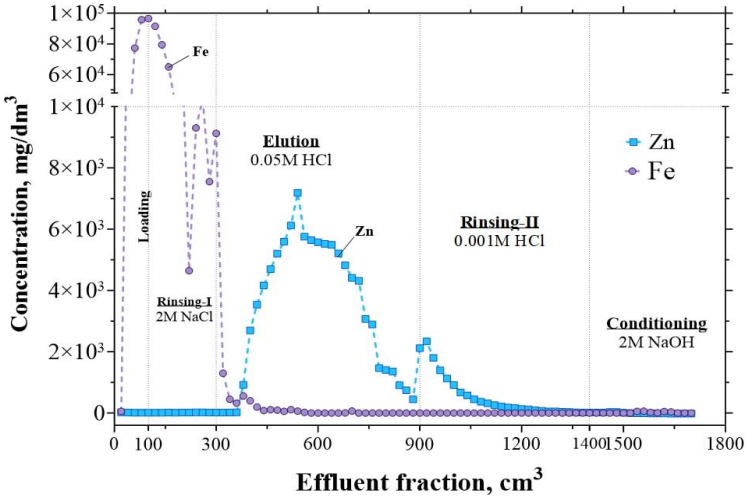

Fig. 6 The main elution curves of the SPL purification procedure (3 BV/h).

The Zn content was fully fixed in the resin from the loaded solution of 2M free NaCl. No leakage could be observed either during the subsequent rinsing step, continued with the same NaCl background. It indicated that this Cl^- ion concentration – provided by the added NaCl – was enough to stabilise the negatively charged chloro-complex zinc species. Meanwhile, virtually all the Fe - previously assured to be in the Fe(II) state - passed through the column. The resin rejects iron in its divalent form in the relatively low Cl^- concentration applied. The elution process removed Zn by adding 0.05 HCl with more volume fraction. It could be expected to be efficient in decomposing the chloro-complex anions of Zn by the distribution behaviour previously confirmed. Although a sharp elution peak of Zn appeared with the applied 0.05 M HCl eluent, a significant tailing also occurred, and the recovery – in the pure section of the eluate – needed some enhancement. Much zinc remained still locked in the column because of – probably - still strong chloro-complexation or some starting hydrolytic precipitation *in situ*. The broad peak of the elution curve for Zn inferred that a relatively dilute eluate could be obtained. Therefore, a second step of elution – or rather second rinsing - with 0.001 M HCl was added to push out the remaining Zn from the resin. Again, a sharp secondary peak followed

by a broad tail curve, indicating that the reason of strong tailing in the first peak was the incomplete decomposition of the sorbable Zn chloro-complex species. Practically all the Zn can be removed with this enhanced elution step. The procedure was repeated by adding also the minor impurities in the loaded solution. Figure 7 shows the complete separation characteristics by the multiple elution peaks. The logarithmic scale of the concentration axis allows to see even the minor peaks clearly.

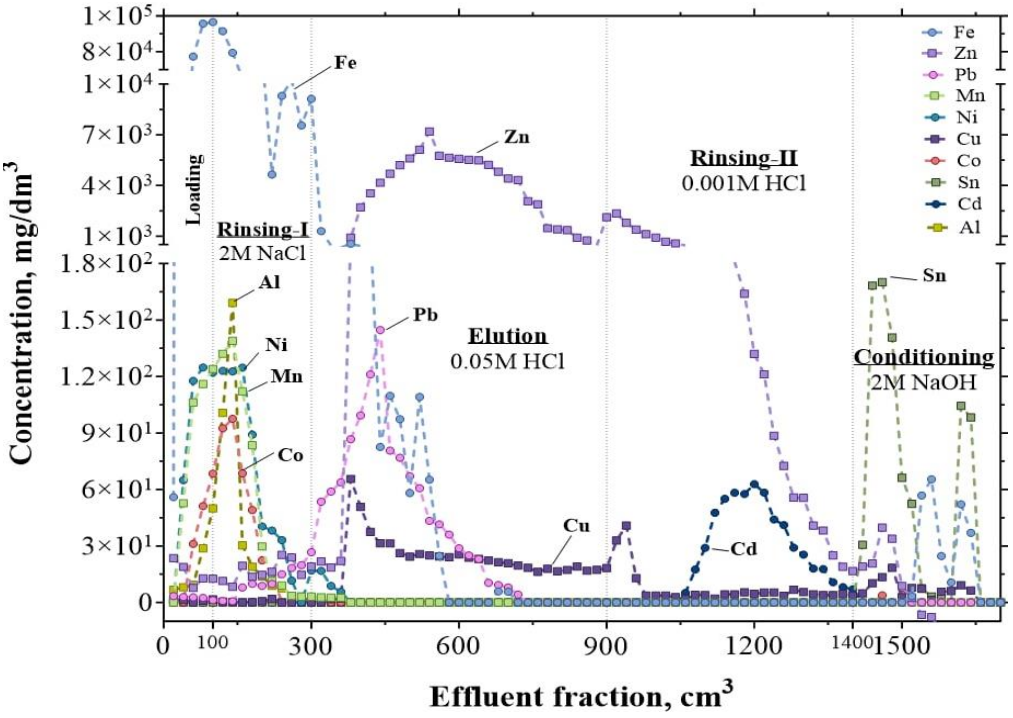

Fig. 7 Elution curves of complete SPL purification to produce pure Zn electrolyte.

According to the distribution functions of several practical or characteristic elements, a large number of potential impurities, like Al, Ni, showing no anion-exchange capability can be separated directly. The same applies to Fe(II), Co(II) and Mn(II), which may form anionic chloro-complexes only at very high Cl^- concentration (> 8 M). All the impurities mentioned above are out of the column before the elution of Zn occurs. Just a few impurities – of negligible importance – may have similar distribution functions to that of Zn. In the main eluate, Pb(II) and Cu(II) appear along with the Zn. Lead contamination, however, is almost excluded by the modern European standards of hot dip galvanising. Similar may be true for cadmium. Cadmium leakage could only be observed at the second elution – rather rinsing - step, and only at the last tail of the Zn elution curve, so this fraction can also be discarded. On the other hand, those impurities which remain strongly fixed in the resin during the elution of Zn, like Sn, will cause no contamination, eluted only at the subsequent conditioning step with – in this case - NaOH. However, the produced dilute Zn solution might pose some challenge for a direct electrodeposition.

The feasibility of an efficient cathodic deposition may require a minimum of 10 ~ 15 g/dm^3 Zn concentration in the chloride electrolyte [25]. To reach even higher Zn concentrations, we tested the hydrolytic precipitation from the purified low-HCl eluate by slightly increasing the pH value, then re-dissolving the separated crystals at the lowest possible level of HCl added (approximately at pH 4~5). In this way, the concentration of the solution can be increased without the necessity of an energy-intensive and time consuming evaporation treatment.

3.2 Derived efficiency characteristics of the separation process

Separation efficiency can be expressed by the elimination/purification ratio (R) [26]:

$$R = \frac{\frac{m_{\mathrm{Me}}^{\mathrm{load}}}{m_{\mathrm{Zn}}^{\mathrm{load}}}}{\frac{m_{\mathrm{Me}}^{\mathrm{elu}}}{m_{\mathrm{Zn}}^{\mathrm{elu}}}} = \frac{m_{\mathrm{Me}}^{\mathrm{load}} \int_{V_s}^{V_e} c_{\mathrm{Zn}} dV}{m_{\mathrm{Zn}}^{\mathrm{load}} \int_{V_s}^{V_e} c_{\mathrm{Me}} dV} \tag{7}$$

Where V_s, is the total effluent volume at the starting point of eluate collection and V_e is at the endpoint. While $m_{\mathrm{Me}}^{\mathrm{load}}$ is the total mass of the loaded and $m_{\mathrm{Me}}^{\mathrm{elu}}$ is the eluted amount of the examined metal, referring to the collected central fraction of the eluate. The analysed concentration (e.g. mg/dm^3) is denoted by c_{Zn} and c_{Me}, respectively. The standard value of the elimination ratio refers to the fraction of the effluent that comprises the central section of the main elution peak of zinc, extending from the point at the half-height on the front (rinsing) side to that of the tail (declining) side.

As another efficiency indicator, the relative amount (m_{Zn}) of Zn recovered in the collected (main) fraction of the eluate from the loaded mass can be expressed by the zinc elution ratio (or zinc yield):

$$E_{\mathrm{Zn}} = \frac{m_{\mathrm{Zn}}^{\mathrm{elu}}}{m_{\mathrm{Zn}}^{\mathrm{load}}} = \frac{\int_{V_s}^{V_e} c_{\mathrm{Zn}} dV}{m_{\mathrm{Zn}}^{\mathrm{load}}} \tag{8}$$

The standard efficiency parameters referring to the elution peaks in Fig. 8 are given in Table 3. The results were obtained by applying a specifically developed computer program for smoothing the elution peaks by the running average method, followed by numerical integration of the concentration curves. The non-sorbable impurities are not included as their removal is considered complete. Most of the practically considerable (or possible) impurities (Al, Co, Ni, Mn, Fe, Cd) of SPL have an overall elimination/purification ratio higher than 1000. This indicates an efficient separation process, producing a pure Zn solution. In contrast, some minor – and practically negligible - impurities (Pb, Cu) characterised by anion exchange distribution functions similar to that of zinc have low elimination ratios, but they are not expected to arise in modern HDG technologies. However, cementation or precipitation techniques can remove these impurities from the purified solution, in other cases.

Table 3 Characteristics of Zn anion-exchange purification procedure shown in Fig. 8

Zn effluent fractions (cm^3)	Standard Zn Yield, E_{Zn}	Standard elimination ratio, R_{std} **R_{std} > 1000 for Al, Co, Ni, Mn and Fe**			
		Fe	Pb	Cu(I)	**Cd**
I. 380-880	0.91	**> 1000**	3.9	3.14	**> 1000**
II. 500-880	0.47	**> 1000**	7.7	2.9	**> 1000**

* The conditioning step is not considered (Sn was fully eluted in the conditioning step)

The section of the effluent in the 380 to 880 cm^3 range can be preferably used directly for electrowinning implying ~ 4 times dilution relative to the loading solution. However, the precipitation and re-dissolution treatment can be easily applied for concentration, even holding some potential for additional purification.

3.3 The main potentiodynamic results

Zinc electrodeposition is generally categorized with high exchange current density values (j_0 > 1.8 −8.8 A/dm^2) and relatively high overpotential to hydrogen [27]. In addition, chloride ions

increase the solution conductivity, the mobility of the Zn species, thereby exerting a virtual depolarization effect on Zn deposition from chloride media, as reported in [28] [29] [30]. Even at the low acid concentration (pH ~ 2), the equilibrium potential of the $2H^+/H_2$ couple is more noble than those values of Zn. As the overpotential shifts the hydrogen reduction to more negative potentials, this danger is mitigated, and in effect Zn is seen deposited.

The ratio of the two parallel currents belonging to either H^+ or Zn^{2+} reduction may express slightly different tendencies at the two extreme pH settings of the examined range of pH 1.5 – 4.5, as can be seen in Fig. 8, referring to a solution of 60 g/dm^3 Zn.

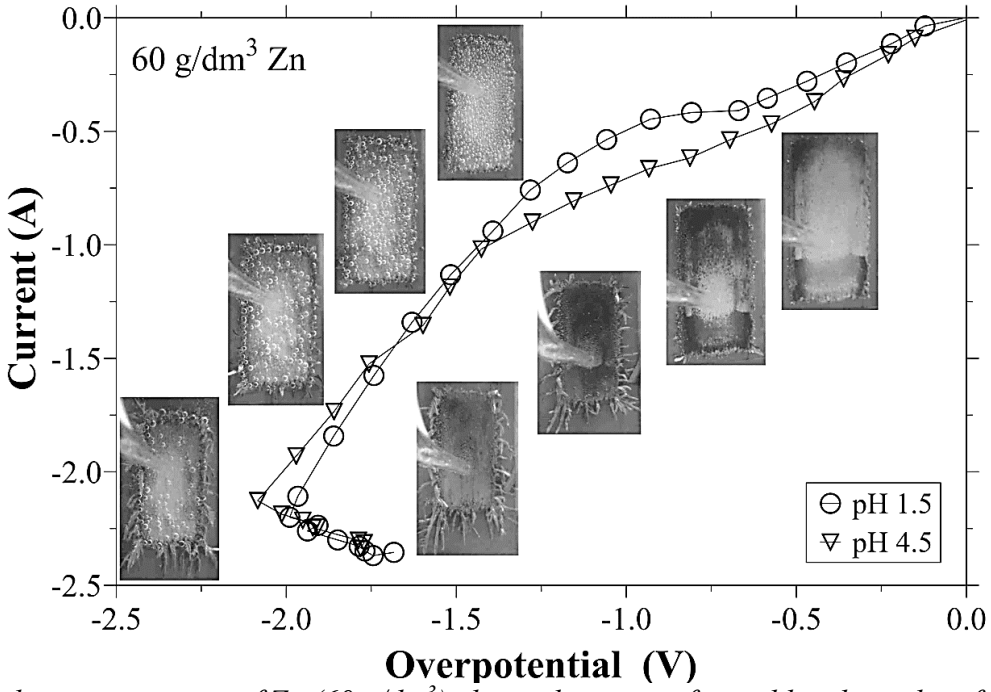

Fig. 8 Polarization curves of Zn (60 g/dm^3) electrodeposition from chloride media of different acid concentrations (pH 1.5 and 4.5).

Starting from the equilibrium (0 V overpotential) in the cathodic direction, the current plots lose their linearity around -0.7 V, where a temporary limiting current density plateau appeared. The incomplete formation of a limiting current infers the beginning of a mixed mechanism. In the electrolyte of the higher H^+ concentration, the initial rise of the current plot can be dominated by the H^+ reduction, which changed for a more dominant Zn^{2+} reduction induced by the roughening of the deposit structure. The virtual plateau is mostly caused by the blocking of the active surface, as the initially formed H_2 bubbles are still attached before growing to the size to be released. Thus the local overpotential is increased while the recorded current is not growing significantly. The series of the photographs on the left show the obvious formation and accumulation of the H_2 bubbles. On the other hand, the plot and the series of photographs belonging to the conditions of pH 4.5 show hardly any effect of H_2 evolution. In this case the reduction of the Zn^{2+} ions may dominate all over the polarization range.

As the overpotential became more negative than -1 V, branchy fern-like dendrites were formed, increasing the actual surface area, thus allowing a faster current increase. Towards the final section of the polarization curve, the electrode surface grew excessively and the local current density dropped sharply, thus more current could be generated by even decreasing overpotentials. This “back-drop” in the potential occurs as the development of the dendritic structure explodes.

Agitation has been seen to homogenize the electrolyte by enhancing the ion transport to the active surface, can increase the effective current, but beyond revealing the nature of the complex electrode processes, it has no real technical possibility to be applied in a conventional production cell.

As the Zn concentration is increased, the polarization curves showed a more constant slope subjected to less hydrogen evolution. This phenomenon is demonstrated by the results shown in Fig. 9. The steeper the slope, the more hydrogen reduction occurs. It is evident from the relevant surface photographs (Fig. 10.*b*) that the more concentrated Zn is in the solution, the more uniform is the metal deposit and the less dendrites are grown at the cathode edges. Therefore, the mass transfer and concentration gradient play essential roles in the deposit macro-morphology. Also the hydrogen evolution reaction has a significant impact on the growth of the dendrites.

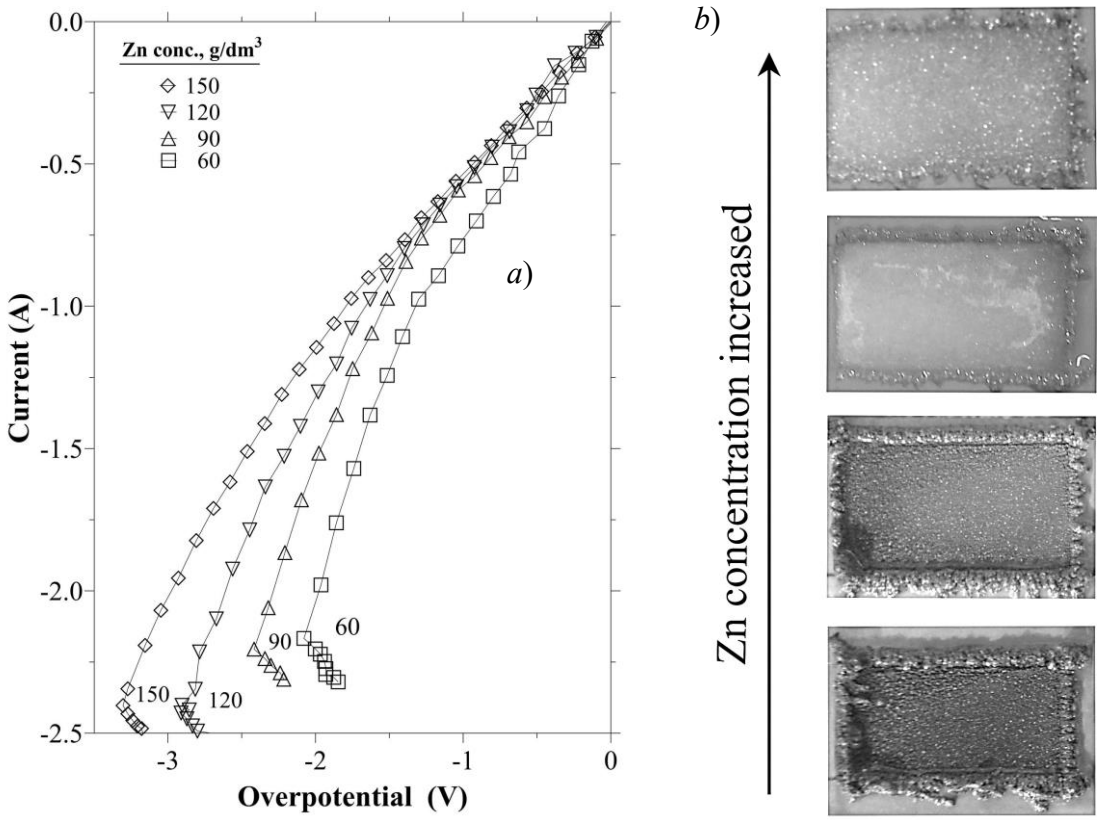

Fig. 9 Polarization curves obtained at different concentrations (a) and the photographs of the obtained final deposits (b) in stationary electrolytes.

3.4 Galvanostatic characteristics

Although the potentiodynamic study has revealed some important characteristics of the cathodic process, actual deposit production by galvanostatic electrowinning experiments were considered necessary to reveal the practical efficiency and morphology characteristics. Primarily, the effects of the initially set pH and the apparent (geometric) current density (c.d.) were examined in various concentration ranges. So as to obtain commensurate deposit masses in all the experimental runs, the same amounts of electric charge (864 As) were supplied to the electrolytic cell. For example, the electrolysis time was 2 h with the 300 A/m^2 setting. In general, as shown by comparing the diagrams in Fig. 10, there is a definite dependence of the current efficiency (c.e.) on the Zn concentration in the stationary electrolyte.

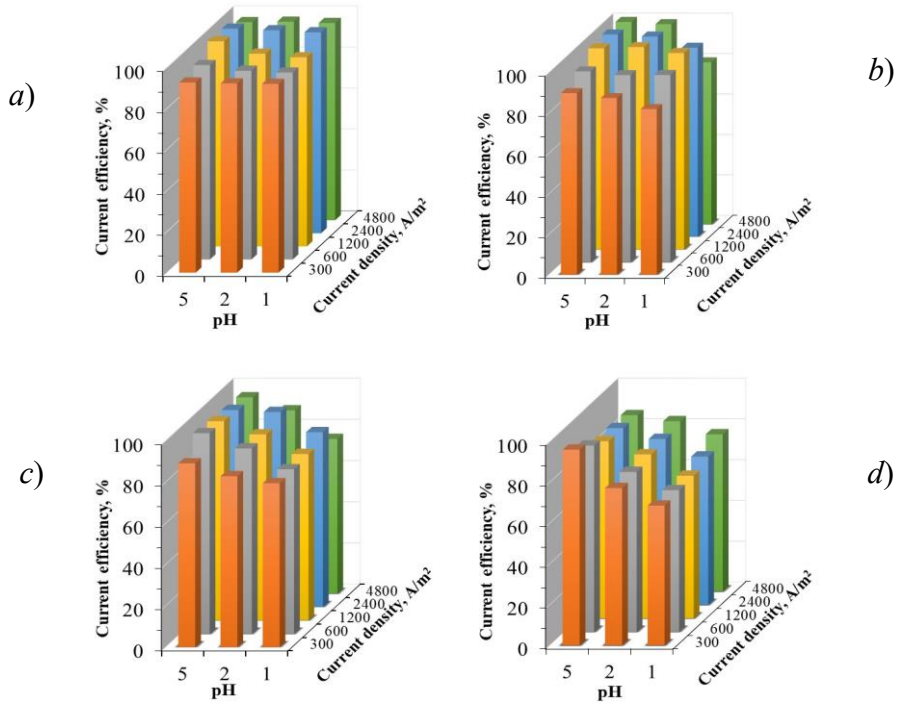

Fig. 10 The current efficiency as the function of the initial pH and the apparent current density with a) 100 g/dm^3, b) 50 g/dm^3, c) 25 g/dm^3, d) 12.5 g/dm^3, Zn in the stationary solution. (charge supplied: 864 As)

Due to the suppression of hydrogen evolution, increasing Zn concentration decreases the secondary cathode reaction of H_2 evolution, which is clearly seen by comparing the average results. Except for the highest Zn concentration (Fig. 11.*a*), decreasing the initial pH could significantly deteriorate the conditions by increasing the ratio of hydrogen evolution in the cathodic current. The electrodeposition from the electrolyte of the highest examined Zn concentration offered an average c.e. above 80%, and the maximum of 99% was reached with pH 5 and 2400 A/m^2 c.d. settings. According to the pH values measured before and after the experiments, a significant oxygen evolution occurred at the inert anode with the starting solution of pH 5. It resulted also in the lowering of the actual pH values during the process. In contrast, with the higher initial acid concentration (pH 1), there was an increase in the pH values, inferring a surplus of hydrogen evolution. In this case the anode reaction must have included a higher ratio of chlorine evolution. Especially with the high (100 g/dm^3) Zn concentration in the chloride electrolyte, the chlorine evolution from the anodic reaction could even be smelled. Any dissolved Cl_2 transported to the cathode may cause corrosion, deteriorating the c.e. mainly influenced by the effect of hydrogen evolution. However, if the availability of Zn species can support higher rates of deposition, increasing the c.d. can increase the current efficiency by outweighing the chemical cathode corrosion. This effect can be noticed in Fig. 11.*a* and *b*. The tendencies continue as the Zn concentration is decreased until 12.5 g/dm^3. However, if the Zn concentration is further reduced, hydrogen evolution becomes dominant and hardly any appreciable efficiency is obtained. The main cathodic process is mostly accompanied by the evolution of H_2. Intensive evolution of H_2 and an associated critically low current efficiency were remarkable if higher apparent current densities were applied with electrolytes of the lowest Zn concentrations.

The examined fundamental parameters also affect the morphology of the obtained deposit. As shown in Fig. 11, no sharply fern-like dendrites were observed in the longer term galvanostatic experiments applying the lowest current density, however quite large dendrites developed in the electrolytes of low Zn-concentration. The structures of the dendrites became finer at higher

current densities. Due to the wider diffusion layers at higher current densities, the dendrites reached further out from the base surface. The protrusions mostly developed at the edges of the cathodes because of the uneven current distribution and the uneven ion supply.

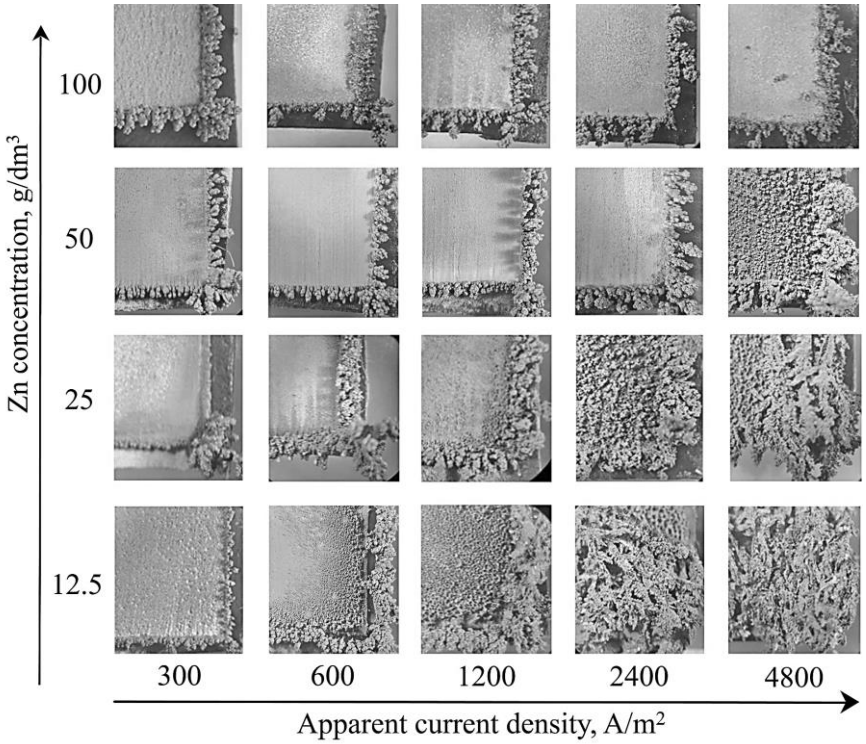

Fig. 11 The morphologies of the deposits obtained with different apparent current densities from electrolytes of different Zn concentrations (initial pH 5).

The changes in the characteristic macro-morphology can be observed at a closer look in Fig. 12, comparing the morphologies obtained at different initial pH settings. Despite the missing agitation of the electrolyte, the tendency of finer crystal structure can be seen again with increased current densities. However, with the pH set close to neutral, the hydroxide precipitation appeared at the higher current densities. Due to the associated H^+ reduction, the local pH may have increased even further, especially at the surface irregularities, where the white precipitation markings appear stronger.

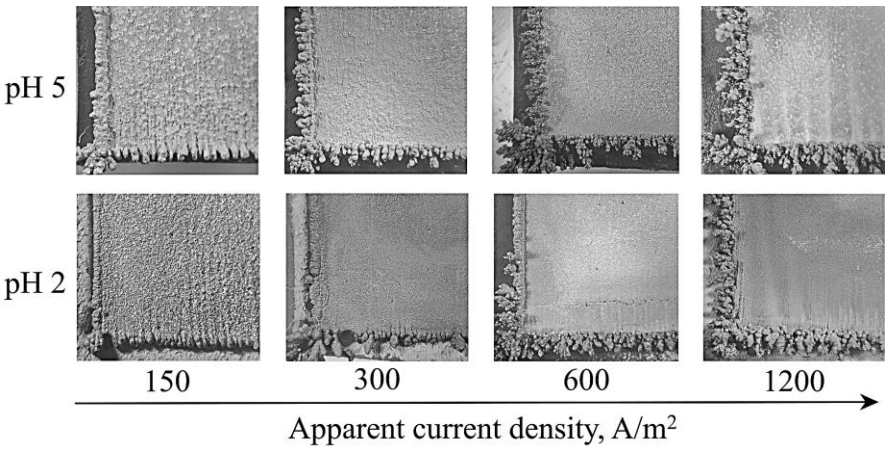

Fig. 12 The surface structures observed on the cathodic deposit from 50 g/dm^3 Zn chloride electrolytes of pH 2 and pH5 at c.d. of 150 – 1200 A/m^2.

The H_2 bubble formation can cause discontinued crystal nucleation, which may develop into small pits at the surface. At lower current densities they may get arranged in lines, by the enhancing effect of micro-cavities available after the rising bubbles leave the original site. However, at higher current densities the free streaming of the gas creates more homogeneous conditions and distributes the electrolyte flow.

The effect of additional NaCl on the electrodeposition of Zn from the chloride media has been studied to characterize the electrolytic characteristics referring to the conditions after the anion-exchange purification of the SPL. It is observed that additional chloride ions affect the morphology and the amount of the Zn deposited. The c.e. values determined are plotted in Fig. 13 as functions of the NaCl concentration added to the originally slightly acidic (pH 3) $ZnCl_2$ solutions, referring to different current densities.

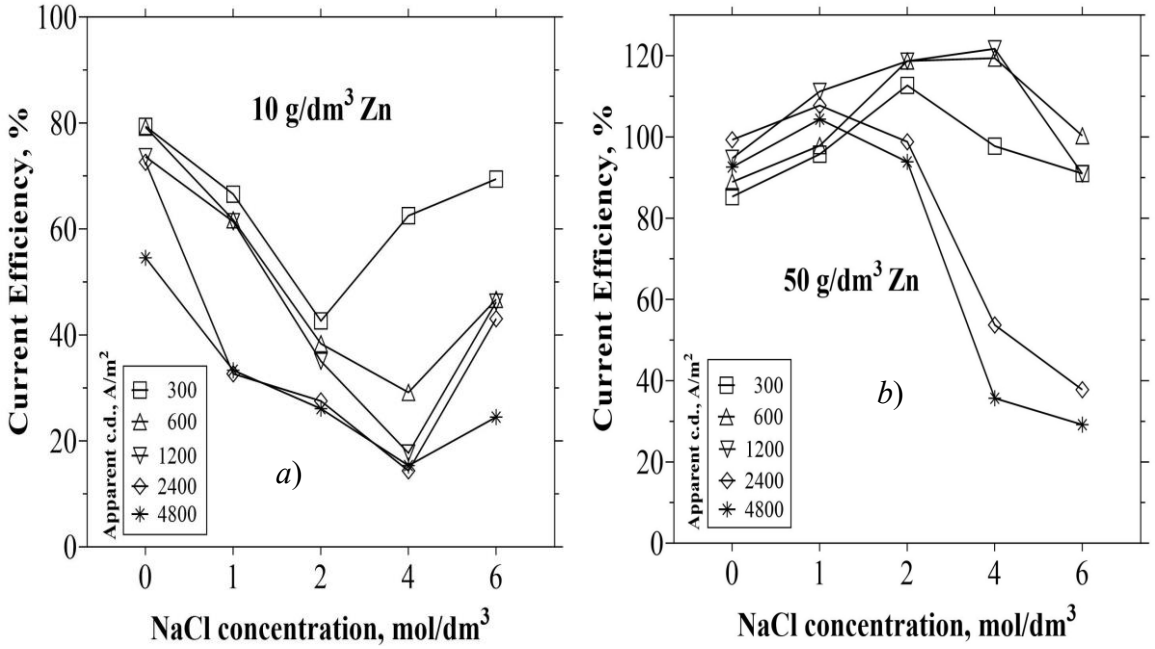

Fig. 13 The current efficiencies as the functions of the added NaCl concentration at different current densities in the 10 g/dm^3 (a) and the 50 g/dm^3 (b) Zn electrolyte (pH 3).

In the electrolyte of the lower (10 g/dm^3) Zn concentration shown in Fig. 14.*a*, the c.e. dropped as the Cl^- ion concentration was increased. The lowest value of 15% was reached with 4M NaCl added to the electrolyte if the highest 2400 – 4800 A/m^2 apparent current densities were applied. The low Zn concentration of the chloride electrolyte gave only loose and spongy deposits, hardly adhering to the substrate, and the addition of NaCl made the conditions even worse. However, further increasing the NaCl concentration beyond 4 mol/dm^3 resulted in slightly increased c.e. values, which can be attributed to the rougher crystal structure of higher actual surface area. In general, this low Zn concentration falls short of practical interest.

In the solution of the higher (50 g/dm^3) Zn concentration (Fig. 14.*b*), the c.e. value continuously increased with the added NaCl in the lower range. The beneficial effect can be attributed to the Na^+ ions, which are more likely to aggregate at Zn metal protrusions, acting as an electrostatic shield, thus minimizing the tip effect of an initial dendrite root [31]. However, the tendency changes at higher NaCl concentrations. The drop of c.e. occurs from lower NaCl additions if the c.d. is higher. This pattern suggests that the Cl^- addition also causes a faster hydrogen evolution by decreasing the availability of the electroactive Zn^{2+} ions by forming chloro-complex species.

The virtual current efficiency results obtained with the electrolytes of the relatively high (50 g/dm^3) Zn concentration in the ranges of 2 – 4 mol/dm^3 NaCl concentrations and 600 – 1200 A/m^2 apparent current densities appeared even surpassing the 100 % level. Due to the rough surfaces, these values were determined from the analyzed difference in the final and the starting Zn concentrations in the solution. The corresponding photographs of the deposits obtained in this range of parameters reveal a visible white coverage of the metallic structure. It is associated with the local increase in the pH caused by an intensive reduction of the H^+ ions.

The final cathode surfaces obtained in the electrolyte of 50 g/dm^3 Zn concentration are shown in Fig. 14 by the array of stereo microscopic photographs of the cathodes referring to different NaCl additions.

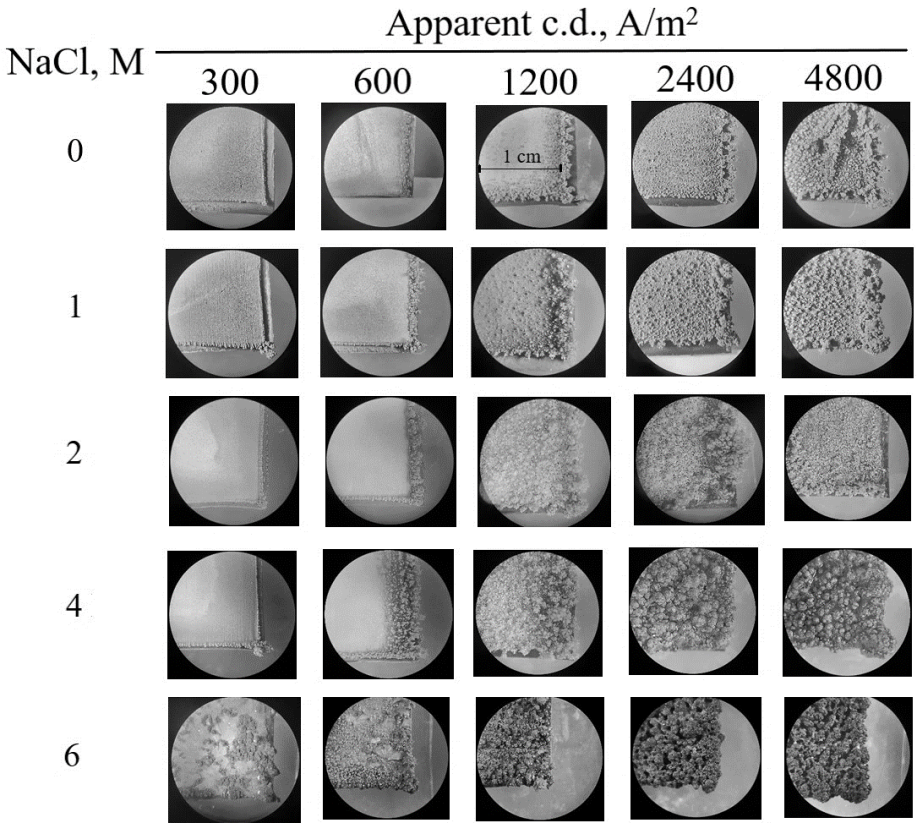

Fig. 14 Comparison of the stereo microscopic pictures of the cathodes obtained with different apparent current densities and NaCl concentrations (50 g/dm^3 Zn).

The highest (2400 and 4800 A/m^2) apparent current densities combined with the highest (4 and 6 M) NaCl additions have developed loose and spongy deposits easily detached from the surface. The resistivity of the deposit became high, also indicated by the increasing cell voltages. The evolution of hydrogen is facilitated by this ragged morphology, which is in line with the obtained extremely low current efficiencies. In these cases, the intensive hydrogen evolution could increase the pH considerably also in the bulk electrolyte, indicating that the side reaction at the cathode associated with the evolution of H_2 can surpass the rate of the regular anodic reaction of oxygen evolution. The balance is made up by the evolution of Cl_2. In this case, the transport of dissolved chlorine to the cathode may also cause corrosion of the deposited metal, further decreasing the efficiency. This extreme condition is confirmed by the strongly increasing bulk pH curves in Fig. 15, exactly mirroring to the dropping c.e. curves in Fig. 13.*b*.

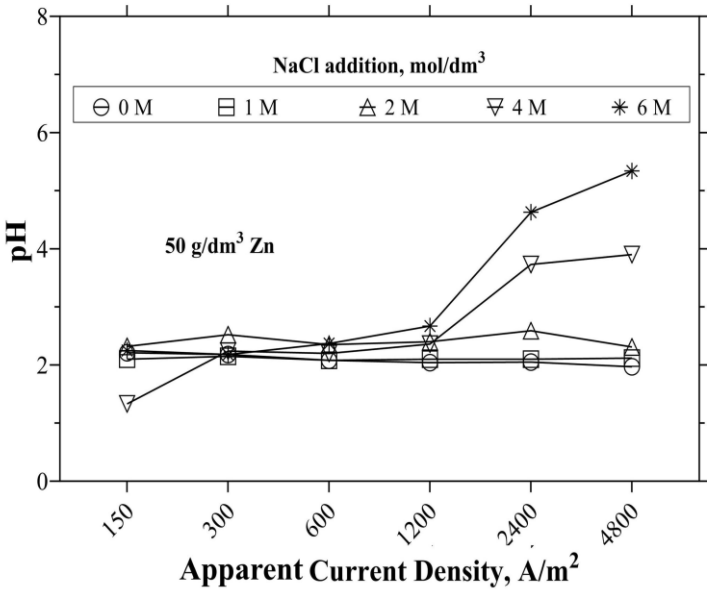

Fig. 15 The final pH values measured in the bulk electrolyte (starting pH 3).

The comparison of the corresponding surface photographs in Figs. 9 and 11 suggests that a moderate addition (1 – 2 M) of NaCl while setting lower current densities (< 600 A/m^2) enhances a denser Zn deposition and suppresses dendrite formation. However, approaching the solubility limit of NaCl could result in the formation of large NaCl crystals. Further increasing the c.d. would divert the deposition towards the edges, resulting in extreme edge thickening and surface roughness. For practical applications, the ranges of higher than 600 A/m^2 c.d. and more than 4 M NaCl concentration should be avoided. Actually, the preliminary anion-exchange purification and evaporation of the real SPL from special de-zincing lines can offer the required Zn and NaCl concentration of the solution, which corresponds to the model solutions found suitable for the efficient electrodeposition.

Li et al. [32] concluded that zinc deposition initially takes place in a regularly arranged crystal structure. The hexagonal closed-packed Zn crystals tend to expose the (002) base plane – parallel to the substrate - thereby minimizing the energy associated with atomic migration. However, as shown in the time series of the pictures in Fig. 16, a heterogeneous growth pattern is developed gradually. With the mass of the deposit increasing, rough globular forms tend to appear over the entire surface, away from the loose structures – of increased electric resistance - at the edges.

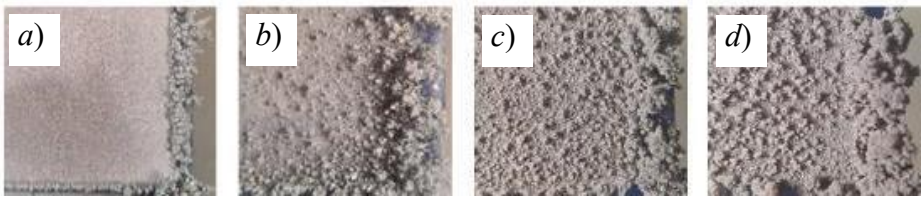

Fig. 16 Observed structures of Zn developed after 5 min (a), 15 min (b), 25 min (c), and 30 min (d) of the electrodeposition (pH 3, 1200 A/m^2, 50 g/dm^3 Zn, 1 M NaCl).

The hexagonally ordered initial growth turns into a non-epitaxial propagation of the crystals, also incurring a subsequent change in the electric field and current distribution. Finally, a non-uniform bulbous surface is produced. At the same time, hydrogen bubbles start forming at the roots of the produced crystals. It causes the weak adherence of the deposit observed when applying the examined highest apparent current densities. If high c.d. is applied, especially in

combination with high NaCl concentrations in the 50 g/dm^3 Zn containing electrolyte, the evolution of hydrogen is also associated with a considerable increase in the pH and the formation of the $Zn(OH)_2$ type precipitate at the roots of the bulbous tips may help disintegrate the structure, causing the detachment and re-dissolution of some Zn metal.

Conclusions

Recovery of metals from spent pickling liquor coming from the galvanizing industry has been widely investigated, but preparing a pure Zn metal from this waste liquor has been out of the conventional topics so far. The previous research in the Laboratory of Chemical Metallurgy, University of Miskolc was concerned with the recovery of pure iron from SPL without further processing of the Zn fraction.

In this research, the SPL coming from the stripping bath has been targeted as a secondary raw material. A novel method to recover pure Zn from SPL has been devised by combining an efficient anion exchange separation, electrolyte preparation and a suitable electrowinning in a simple open cell. Iron and all the practically important other impurities can be eliminated from the chloride solution containing also NaCl, followed by de efficient electrodeposition of pure Zn. Both the anion-exchange separation and the galvanostatic electrodeposition of Zn could be carried out by using only conventional equipment, but finely adjusting the main operating parameters. The efficiency characteristics are remarkable. The major effects in the chloride media also replacing HCl with NaCl where possible were interpreted. The proposed technique offers minimizing the environmental issue caused by SPL, while adding extra value to the recovered metal, fulfilling the modern requirements of SPL regeneration.

New scientific results

C1. Claims on the Zn electrolyte purification by AIEX

C1.1. The replacement of HCl by NaCl provides similar anion-exchange tendencies of zinc and iron, by just slightly decreasing the maximum distribution coefficient of Zn occurring at 2-2.25 M free Cl^- concentration. Any type of strongly basic quaternary amine anion-exchange resin can be used. The new equilibrium distribution functions are presented in the figure below.

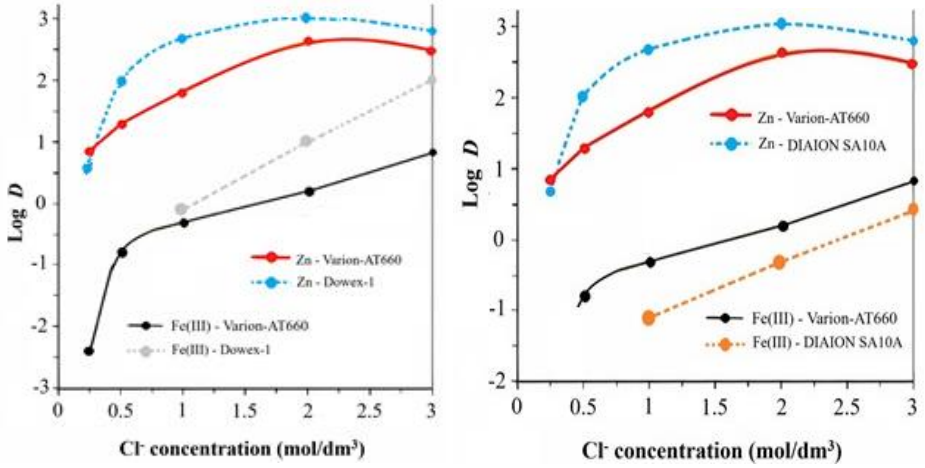

The anion-exchange distribution coefficients of Zn(II) and Fe(III) as functions of the added NaCl concentration, applying different brands of strongly basic resins. (solid lines – actual experiments with NaCl, dashed lines – ref. [33] [34] *with HCl)*

C1.2. Iron, as the main impurity, is hard to separate from Zn in the trivalent state. Therefore, the process is effective after reducing the contained Fe(III) to Fe(II) by the com-proportionation reaction, using powdered or granulated iron (mild steel). After this pre-treatment, any appreciable anion-exchange sorption of iron is avoided at the free Cl^- concentration where Zn is strongly sorbed.

C1.3. The loading of the SPL and the first rinsing step can be carried out with ~ 2 M NaCl solutions, but the elution of Zn should be carried out with a ~ 0.05 M HCl eluent. Further reducing the HCl concentration to 0.001 M can improve the Zn elution and still avoids hydrolytic precipitation, but any Cd impurity is also released from the resin. A 1 - 2 bed volumes/hour (BV/h) flow rate should be generally applied, and lower flow rates can produce better separations.

C1.4. The optimised anion-exchange purification procedure is shown below.

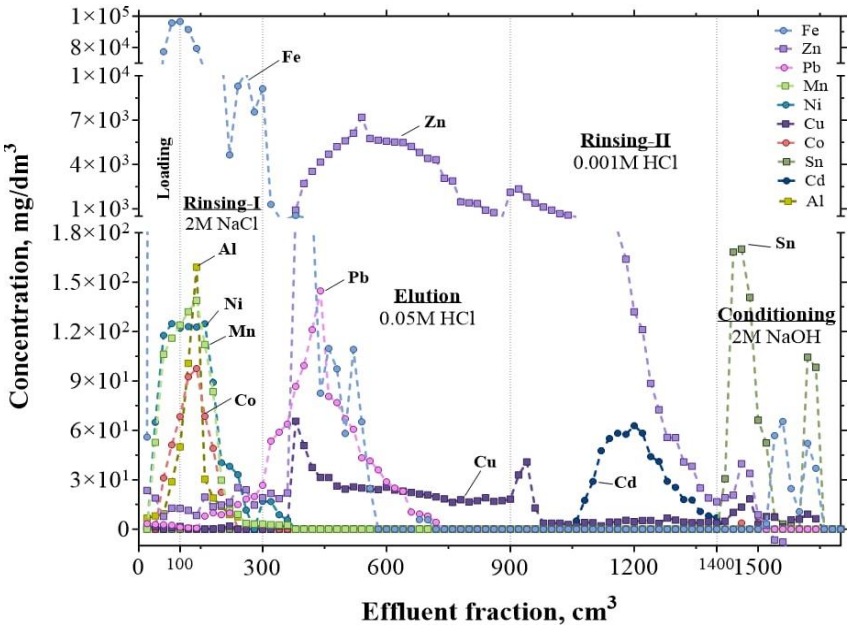

The optimised anion-exchange separation procedure.

This procedure can offer close to 1000 standard purification ratios for Zn in the SPL referring to the main impurities of Fe, Al, Ni, Co, Cd, Mn, and Sn while the yield of Zn is higher than 90 %. The purification ratios of Pb and Cu are however just around 3 – 4. These elements are practically negligible in the SPL, or they can be eliminated by cementation, if required.

C2. Claims on the characteristics of Zn electrodeposition from chloride media

C2.1. In the stationary solution corresponding to the purified SPL (~ 50 g/dm^3 Zn, pH~2) cathodic polarization develops first a limiting current plateau around -0.7 - -1 V. The initial rise of the current is dominated by the H^+ reduction. The current plateau is caused by the blocking of the active surface, as the initially formed H_2 bubbles are still attached before growing to the size to be released, it is followed by a more dominant Zn^{2+} reduction induced by the roughening of the deposit. The interlinked phenomena are demonstrated in the figure below.

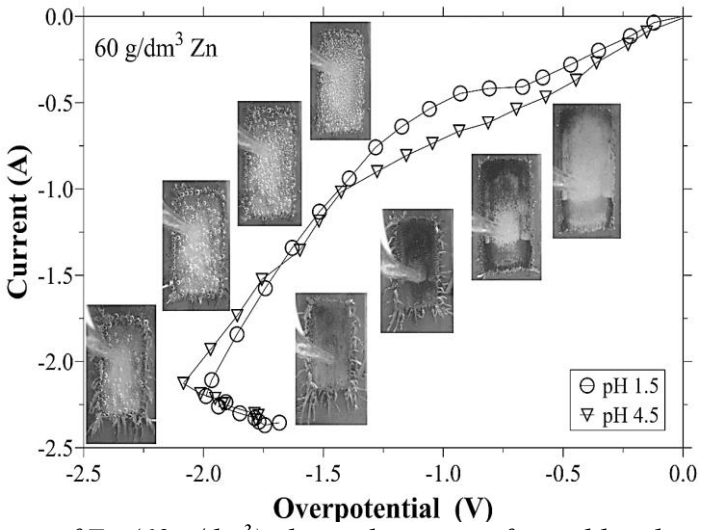

Polarization curves of Zn (60 g/dm^3) electrodeposition from chloride media of different acid concentrations (pH 1.5 and 4.5).

C2.2. Increasing the Zn concentration (even beyond 60 g/dm^3) depresses the H_2 evolution significantly. The electrode surface is less blocked by gas bubbles, thus the effective current density is reduced, while the Zn supply to the surface by the natural diffusion is also increased. This combined effect results in a more uniform zinc deposit and less dendrites grown at the cathode edges. The supply of the electroactive zinc species at the electrode interface plays a decisive role in the deposit macro-morphology.

C2.3. Contaminating the SPL electrolyte with Fe and Ni in the (~ 1 g/dm^3 range), hydrogen evolution will increase because of its lower overpotential to both elements. However, the generated gas bubbles – until released – block the actual site, inhibiting the further preferential deposition and allowing zinc of higher hydrogen overpotential to continue depositing. This kinetic phenomenon is behind the "anomalous" electrodeposition from a mixed solution. At increased concentrations of these impurities, the dendrites at the edges of the cathode are getting not just fewer but also shorter.

C2.4. In high ranges of Fe concentration (30 – 60 g/dm^3), the intensive generation of hydrogen bubbles agitates the electrolyte solution in the vicinity of the cathode surface. This agitating effect promotes Zn deposition but later it is outweighed by the chemical effect of the increasing local pH. It may trigger a local formation of hydroxide particles, hindering the deposition of the less noble zinc. Iron deposition results in more contaminated zinc deposits.

C3. Claims on the efficiency of Zn electrowinning from purified chloride solution

C3.1. The electrodeposition from the electrolyte of the highest examined Zn concentration (100 g/dm^3) offers an average current efficiency ~ 90% in the pH 1 – 5 and the current density of 300 – 4800 A/m^2 range. The maximum of ~ 99% can be reached with pH 5 and 1200 - 2400 A/m^2 settings. On the other hand, at the lowest examined Zn concentration (12.5 g/dm^3), the corresponding average is about 20 % lower. The reduction of H^+ ions at higher current densities can raise the local pH, especially at the irregularities, where hydroxide precipitation appears. The characteristics are graphically shown below.

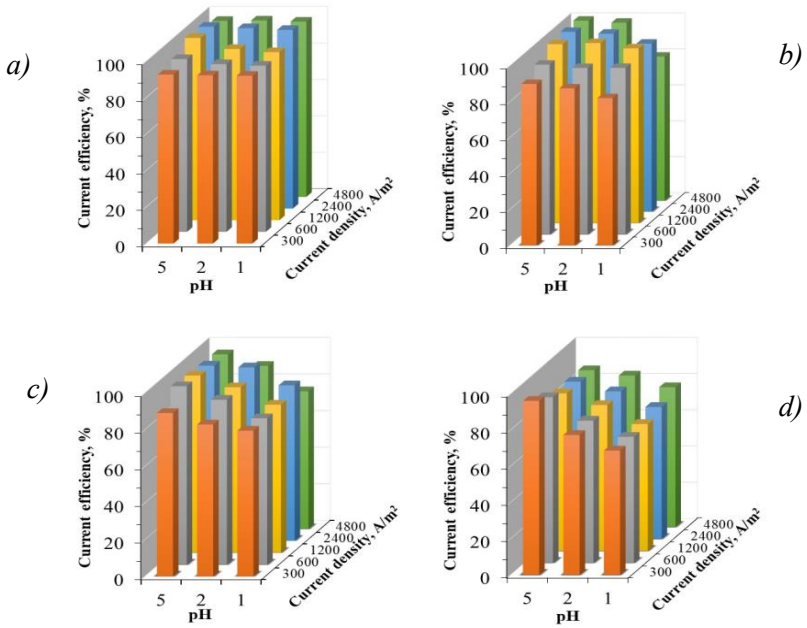

The current efficiency as the function of the initial pH and the apparent current density with a) 100 g/dm^3, b) 50 g/dm3, c) 25 g/dm^3, d) 12.5 g/dm^3, Zn in the stationary solution. (charge supplied: 864 As).

C3.2. Dendrite formation is promoted by higher current densities and lower Zn-concentrations in the bulk electrolyte. Due to the depletion of electroactive Zn species in the vicinity of the cathode surface, dendrites grow further out from the base surface. The protrusions mostly develop at the edges of the cathode because of the uneven current distribution, due to the skin effect of the electron density in the metal and the preferential ion supply around the edges of the electrode in a stationary solution.

C3.3. Due to the oxygen evolution at the inert anode, the initial pH 5 values decrease in the practically high Zn-containing electrolyte. However, with significant initial acid concentration (pH 1), this tendency is reversed by the surplus of hydrogen evolution at the cathode. In this case the anode reaction includes a sensible ratio of chlorine evolution. This is the second reason why the pH must be controlled.

C3.4. In the practically feasible 50 g/dm^3 Zn – pH3 stationary electrolyte, the current efficiency increases with the additional Cl^- ions in the 0 – 4 M NaCl range, especially with moderate (< ~ 1000 A/m^2) current densities. The beneficial effect is attributed to the Na^+ ions, which are more likely to aggregate around the protrusions. However, this effect is reversed if further NaCl is added, caused by the high salt concentration, which increases the viscosity and decreases the transport of the electroactive species to maintain the required current. The virtual current efficiency may appear beyond 100% in the medium range, which is associated with the local increase in the pH caused by an intensive reduction of the H^+ ions, causing precipitation. On the other hand, in the electrolyte of critically low (~ 10 g/dm^3) Zn concentration, the current efficiency drops sharply as the Cl^- ion concentration is increased. Under these conditions, only loose and spongy deposits, just weakly adhering to the substrate, arise.

List of relevant publications

Journal Articles

1. H. Zakiyya, I. B. Illés and T. Kékesi, "*Interpreting the main effects on the efficiency and morphology for establishing a procedure of electrodepositing Zn from purified chloride SPL solutions*," *Springer Nature, App. Sci*. 2024 (under-revision)
2. H. Zakiyya and T. Kékesi, "*Potentiodynamic study of the effects of nickel on the electrodeposition of zinc from chloride media*," *Int. J. Eng. Manage. Sci.*, vol. 8, no. 2, pp. 15-22, 2023. doi:10.21791/IJEMS.2023.2.2
3. H. Zakiyya and T. Kékesi, "*Preliminary study of pure zinc from spent pickling liquor by combining anion exchange and electrodeposition*," Hungarian Materials Science and Engineering, vol. 47, no. 1, pp. 88-99, 2023
4. H. Zakiyya and T. Kékesi, "Anion exchange separations to produce a suitable electrolyte for the electrodeposition of pure zinc," *Multidisciplinary Sciences* vol. 12, no.3, pp. 127-138, 2022. doi:10.35925/j.multi.2022.3.12

Conference Proceedings

1. H. Zakiyya and T. Kékesi, "Potentiodynamic characteristic of zinc electrodeposition from chloride solution," *MultiScience – XXXIII. MicroCAD Multidisciplinary Scientific Conference,* University of Miskolc, 23-24 May, 2019. ISBN 978-963-358-177-3
2. H. Zakiyya and T. Kékesi, "Spent pickling liquor as industrial waste recover opportunities" LIMBRA Ed. Bartha et al.: *Entrepreneurship in the raw materials sector* –ISBN: 978-1-032-19596-4
3. H. Zakiyya and T. Kékesi, "The effect of Fe impurity on the electrodeposition of Zn from spent pickling liquor" ISDM-TU Bergakademie Freiberg

Periodical Articles

1. H. Zakiyya, I. B. Illés and T. Kékesi, "Determination of optimum chromatographic parameters for the anion-exchange separation process to prepare a Zn electrolyte from the spent pickling liquor" *Almanach-of PhD Students*, Faculty of Materials and Chemical Engineering, University of Miskolc, vol.1, pp. 41-48, 2023. ISSN 2939-7294
2. H. Zakiyya and T. Kékesi, "The effect of main parameters on the electrodeposition of Zn from HCl solutions" *Almanach of PhD Students*, Faculty of Materials and Chemical Engineering, University of Miskolc, vol.1, pp. 76-81, 2022. ISSN 2939-7294

Oral Presentations

1. H. Zakiyya and T. Kékesi, "*Potentiodynamic characteristic of zinc electrodeposition from chloride solution*," MultiScience – XXXIII. MicroCAD Multidisciplinary Scientific Conference, University of Miskolc, 23-24 May, 2019. ISBN 978-963-358-177-3
2. H. Zakiyya and T. Kékesi, "*The importance of preliminary purification process of spent pickling liquor*" 16th Miklos Ivanyi International PhD-DLA Symposium- 26-27 October 2021, Pecs, Hungary
3. H. Zakiyya and T. Kékesi, "*Spent pickling liquor as industrial waste recover opportunities*," LIMBRA: International scientific conference on entrepreneurship in the raw materials sector – 24 November 2021, University of Miskolc, Hungary

4. H. Zakiyya and T. Kékesi, "*The potential processes to recover metals from spent pickling liquor"* International Jubilee Interdisciplinary doctoral student conference (IDK2021) – 12 November 2021, University of Pecs, Hungary
5. H. Zakiyya and T. Kékesi, "*Anion exchange separations to produce a suitable electrolyte for the electrodeposition of pure zinc*" MultiScience – XXXV. microCAD International Multidisciplinary Scientific Conference*,* 13-14 October 2022, University of Miskolc, Hungary
6. H. Zakiyya and T. Kékesi, "*The recovery of Zn from SPL by combining anion-exchange separation and electrodeposition in chloride solutions*" MTA Committee of Metallurgy, Hungary, 13 December 2022, NAGEV CINK Kft. Ócsa, Hungary
7. H. Zakiyya and T. Kékesi, "*The recovery of pure Zn from SPL by combining electrowinning and aqueous separation process*" Hungarian Science Day, 10 November 2022, Miskolc, Hungary
8. H. Zakiyya and T. Kékesi, "*The potentiodynamic characteristic of iron in the Zn electrodeposition from chloride media*" Digital presentation – 242nd Electrochemical Society Meeting*,* 9-13 October 2022, Atlanta Hilton, Georgia, USA.
9. H. Zakiyya and T. Kékesi, "*Optimization of anion-exchange separation to produce pure Zn electrolyte from spent pickling liquors*" 224th Electrochemical Society Meeting*,* 10 October 2023, Gothenburg, Sweden.
10. H. Zakiyya and T. Kékesi, "*Optimization of anion-exchange separation to produce pure Zn electrolyte from spent pickling liquors*" [elevation pitch] 224th Electrochemical Society Meeting*,* 9 October 2023, Gothenburg, Sweden.
11. H. Zakiyya and T. Kékesi, "*The effect of Fe impurity on the electrodeposition of Zn from spent pickling liquo*r" International Student Day of Metallurgy, 11 April 2024, TU Bergakademie Freiberg, Germany.

References

[1] G. Kong and R. White, "Toward cleaner production of hot dip galvanizing industry in China," *J. Clean. Prod.,* vol. 18, no. 10-11, pp. 1092-1099, 2010. doi:10.1016/j.jclepro.2010.03.006.

[2] M. Dong, X. Xue, A. Kumar, H. Yang, M. I. Sayyed, S. Liu and E. Bu, "A novel method of utilization of hot dip galvanizing slag using the heat waste from itself for protection from radiation," *J. Hazard. Mater.,* vol. 344, pp. 602-614, 2017. doi:10.1016/j.jhazmat.2017.10.066.

[3] V. Kuklík and J. Kudláček, "Hot-dip galvanizing and the environment," in *Hot-dip galvanizing of steel structure*, Oxford, Butterworth-Heinemann is an imprint of Elsevier, 2016. doi:10.1016/B978-0-08-100753-2.00013-6, pp. 199-202.

[4] American Galvanizer Association, "Hot-Dip Galvanized Steel for Power Infrastructure: Hot-Dip Galvanizing (HDG) Process," American Galvanizer Association, June 2018. [Online]. Available: https://galvanizeit.org/hot-dip-galvanized-steel-for-power-infrastructure/hot-dip-galvanizing-hdg-process. [Accessed 3 January 2019].

[5] M. Regel-Rosocka, L. Nowak and M. Wisniewski, "Removal of zinc(II) and iron ions from chloride solutions with phosphonium ionic liquids," *Sep. Purif. Technol.,* vol. 97, pp. 158-163, 2012. doi: 10.1016/j.seppur.2012.01.035.

[6] A. Anderez, F. J. Alguacil and F. A. Lopez, "Acid pickling of carbon steel," *Rev. de Metal.,* vol. 58, no. 3, pp. 1-11, 2022. doi:10.3989/revmetalm.226.

[7] L. Pietrelli, S. Ferro and M. Vocciante, "Raw materials recovery from spent hydrochloric acid-based galvanizing," *Chem. Eng. J.,* vol. 341, no. December 2017, pp. 539-546, 2018. doi:10.1016/j.cej.2018.02.041.

[8] V. Kuklik and J. Kudlacek, "Chemical pre-treatment," in *Hot-Dip Galvanizing of Steel Structures*, Oxford, UK, Butterworth-Heinemann is an imprint of Elsevier, 2016. doi:10.1016/B978-0-08-100753-2.00003-3, pp. 17-27.

[9] Y. Xu, Y. Zhang, Y. Shu, H. Song, X. Shu, Y. Ma, L. Hao, X. Zhang, X. Ren, Z. Wang and X. Zhang, "Composition and leaching toxicity of hydrochloric acid pickling sludge generated from the hot-dip galvanized steel industry," *ACS Omega,* vol. 7, no. 16, pp. 13826-13840, 2022. doi:10.1021/acsomega.2c00121.

[10] M. Regel-Rosocka, "A review on methods of regeneration of spent pickling solutions from steel processing," *J. Hazard. Mater.,* vol. 177, no. 1-3, pp. 57-69, 2010. doi:10.1016/j.jhazmat.2009.12.043.

[11] J. Carrillo-Abad, M. Garcia-Gabaldon and V. Perez-Herranz, "Treatment of spent pickling baths coming from hot dip galvanizing by means of an electrochemical membrane reactor," *Desalination,* vol. 343, pp. 38-47, 2014. doi:10.1016/j.desal.2013.11.040.

[12] A. Argawal and K. Sahu, "An overview of the recovery of acid from spent acidic solutions from steel and electroplating industries," *J. Hazard. Mater.,* vol. 171, no. 1-3, pp. 61-75, 2009. doi:10.1016/j.jhazmat.2009.06.099.

[13] R. Gueccia, W. Daniel, S. Randazzo, A. Cipollina, J. Koschikowski and G. D. Micale, "An integrated approach for the HCl and metals recovery from waste pickling solutions: pilot plant and design operations," *Chem. Eng. Res. Des.,* vol. 168, pp. 383-396, 2021. doi:10.1016/j.cherd.2021.02.016.

[14] A. Arguillarena, M. Margallo, A.-F. Axel, J. Pinedo, P. Gomez, I. Ortiz and A. Urtiaga, "Circular economy in hot-dip galvanizing with zinc and iron recovery from spent pickling acids," *RSC Adv.,* vol. 13, no. 10, pp. 6481-6489, 2023. doi:10.1039/d2ra08195d.

[15] A. Devi, A. Singhal, R. Gupta and P. Panzade, "A study on treatment methods of spent pickling liquor generated by pickling process of steel," *Clean Technol. Environ. Policy,* vol. 16, no. 8, pp. 1515-1527, 2014. doi:10.1007/s10098-014-0726-7.

[16] G. Leonzio, "Recovery of metal sulphates and hydrochloric acid from spent pickling liquors," *J. Clean. Prod.,* vol. 129, pp. 417-426, 2016. doi:10.1016/j.jclepro.2016.04.037.

[17] The Europen Parliament and the Council of the European Union, "EUR-Lex Access to European law - Directive (EU) 2018/851 of the European Parliament and of the Council of 30 May 2018 amending Directive 2008/98/EC on waste," Eurpen Union, 30 May 2018. [Online]. Available: https://eur-lex.europa.eu/legal-content/EN/TXT/?uri=CELEX:32018L0851. [Accessed 20 September 2023].

[18] I. Ortiz, E. Bringas, H. Samaniego and M. F. S. Roman, "Membrane processes for the efficient recovery of anionic pollutants," *Desalination,* vol. 193, no. 1-3, pp. 375-380, 2006. doi:10.1016/j.desal.2005.05.034.

[19] M. Kaya, S. Hussaini and S. Kursunoglu, "Critical review on secondary zinc resources and their recycling technologies," *Hydrometallurgy,* vol. 195, no. April, p. 105362, 2020. doi:10.1016/j.hydromet.2020.105362.

[20] Bureau of International Recycling, "Report on the environmental benefits of recycling - 2016 edition," BIR, Brussel, 2016.

[21] Sigma Aldrich, "Material Science Product," Sigma Aldrich, 2018. [Online]. Available: https://www.sigmaaldrich.com/materials-science/material-science-product.html?TablePage=111535999.. [Accessed 11 January 2019].

[22] S. T. Ali, K. S. Rao, C. Laxman, N. R. Muniratham and T. L. Prakash, "Preparation of high pure zinc for electronic applications using selective evaporation under vacuum," *Sep. Purif. Technol.,* vol. 85, pp. 178-182, 2012. doi:10.1016/j.seppur.2011.10.009.

[23] A. Moezzi, A. M. McDonagh and M. B. Cortie, "Zinc oxide particle: Synthesis, properties and applications," *Chem. Eng. J.,* Vols. 185-186, pp. 1-22, 2012. doi:10.1016/j.cej.2012.01.076.

[24] G. Bao , Q. Fan, D. Ge, K. Wang, M. Sun, Z. Zhang, H. Guo, H. Yang, B. He and Y. Zheng, "In vitro and in vivo studies to evaluate the feasibility of Zn-0.1Li and Zn-0.8Mg application in the uterine cavity microenvironment compared to pure zinc," *Acta. Biomater.,* vol. 123, pp. 393-406, 2021. doi:10.1016/j.actbio.2020.12.048.

[25] D. J. Mackinnon, J. M. Brannen and R. M. Morrison, "Zinc electrowinning from aqueous chloride electrolyte," *Journal of Applied Electrochemistry,* vol. 12, pp. 39-53, 1982.

[26] T. Kékesi, A novel method of copper purification by anion-exchange in chloride media, Tohoku University, Sendai, Japan: PhD thesis., 1994.

[27] N. D. Nikolić, "A Review: Influence of the exchange current density and overpotential for hydrogen evolution reaction on the shape of electrolytically produced disperse forms," *J. Electrochem. Sci. Eng.,* vol. 10, no. 2, pp. 111-126, 2020. https://doi.org/10.5599/jese.707.

[28] K. Keisuke, S. Oue and H. Nakano, "Effect of chloride ions in electrowinning solutions on zinc deposition behavior and crystal texture," *Mater. Trans.,* vol. 58, no. 10, pp. 1418-1426, 2017. https://doi.org/10.2320/matertrans.M-M2017827.

[29] D. J. Mackinnon and J. M. Brannen, "Zinc deposit structures obtain from synthetic zinc chloride electrolyte," *J. App. Electrochem.,* vol. 9, pp. 603-613, 1979. https://doi.org/10.1007/BF00610948.

[30] M. Nicol, C. Akilan, V. Tjandrawan and J. A. Gonzalez, "The effect of halides in the electrowinning of zinc . II . Corrosion of lead-silver anodes," *Hydrometallurgy,* vol. 173, no. May, pp. 178-191, 2017. https://doi.org/10.1016/j.hydromet.2017.08.017.

[31] F. Wan, L. Zhang, X. Dai, X. Wang , Z. Niu and J. Chen, "Aqueous rechargeable zinc/sodium vanadate batteries with enhanced performance from simultaneous insertion of dual carriers," *Nature Communications,* vol. 9, no. 1, pp. 1-11, 2018. https://doi.org/10.1038/s41467-018-04060-8.

[32] Z. Li and A. W. Robertson, "Electrolyte engineering strategies for regulation of the Zn metal anode in aqueous Zn-ion batteries," *Battery Energy,* vol. 2, no. 1, pp. 1-30, 2022. https://doi.org/10.1002/bte2.20220029.

[33] T. Kekesi, K. Mimura and M. Isshiki, "Ultra-high purification of iron by anion exchange in hydrochloric acid solutions," *Hydrometallurgy,* vol. 63, no. 1, pp. 1-13, 2002. doi:10.1016/S0304-386X(01)00208-0.

[34] T. Kekesi and M. Isshiki, "Anion Exchange for Ultra-High Purification of Transition Metals," *ERZMETALL,* vol. 56, no. 2, pp. 59-67, 2003.